Real-Time State Anxiety Estimation for Adaptive Wearable Exoskeleton Control

Mahta Akhyani, Pilwon Hur*

Department of Mechanical and Robotics Engineering, GIST

(E-mail: mahta.akhyani@gm.gist.ac.kr, pilwonhur@gist.ac.kr)

Abstract In rehabilitation exoskeletons, physical coupling transforms every actuation error into a proprioceptive event that triggers state anxiety before any trust measure registers a change. This paper presents a closed-form computational model of state anxiety computable in real time from kinematic and cardiac signals already available in wearable human-robot interaction (HRI) systems. The model integrates precision-weighted prediction error, sigmoidal cardiac recovery, and negativity bias into a single scalar suitable for closed-loop adaptive control. Parameter ranges are verified against acute psychosocial stress data and published cardiac recovery timescales [6]. $A(t)$ updates at the cardiac sampling rate with ∼3–5 s detection latency from a kinematic error event — well below the minute-scale dynamics of trust failure.

Keywords wearable robotics, exoskeleton, state anxiety, human-robot interaction, closed-loop control, heart rate response

1. Introduction

Trust in wearable HRI fails differently from trust in detached automation. An exoskeleton applies forces directly to the wearer's body. Errors occur within the peripersonal space, where threat sensitivity is highest. Timing errors as small as 2.8% of a stride period are perceptually detectable [1]. Existing trust models in HRI operate at the outcome layer: they quantify the resulting trust state, from behavioural or self-report measures, without representing the upstream physiological cascade.

In HRI outside the exoskeleton context, state anxiety mediates dispositional to learned trust [2], most strongly without a performance history. The mechanism transfers to wearable HRI: sensorimotor prediction error (SPE) produces state anxiety [3], which increases sensory precision weighting and amplifies subsequent mismatches [7]. This loop closes before any trust outcome is observable. Modelling anxiety (the mechanism) rather than trust (the outcome) is therefore the prerequisite for real-time intervention in physical HRI. This paper contributes (i) a closed-form, real-time state anxiety model driven by kinematic prediction error and cardiac recovery, (ii) parameter-range verification against acute-stress and cardiac-recovery data, and (iii) a closed-loop architecture using the estimate to adapt actuation predictability before trust failure.

2. Computational Model of State Anxiety

2.1 Model Structure

State anxiety at time t is modelled as:

$$A(t) = A_{\mathrm{base}} + \sum_i w_i \cdot U_i \cdot \frac{\mathrm{HRS}(t - t_i) - \mathrm{HRS}_\infty}{\mathrm{HRS}_0 - \mathrm{HRS}_\infty} \quad (1)$$

The index i runs over stressor events up to time t; t_i is the onset time of event i. A_{base} is the individual's baseline (STAI trait score). U_i is the unexpectedness of event i, motivated by precision-weighting accounts of anxiety [7] and defined in Section 2.3. The normalized HRS fraction discounts each event by recovery progress since t_i. Motivated by the negativity bias literature [4], we set $w_i = 2.5$ for error events and $w_i = 1.0$ for neutral ones; the ratio is a design choice to be refined through per-subject fitting. A perfectly anticipated event contributes near-zero: anxiety responds to unpredictability, not magnitude.

2.2 Heart Rate Response Function

Sympathetic activity decays exponentially after stressor offset:

$$S(t) = S_i + (S_0 - S_i)\, e^{-t/T_s} \quad (2)$$

At onset t_i, S is reset to S_0; the step assumption holds because sympathetic onset is sub-second relative to T_s on the order of minutes. Heart rate response is a sigmoidal saturation of $S(t)$, reflecting the compression of cardiac chronotropic response at high sympathetic drive:

$$\mathrm{HRS}(t) = 1 + M \cdot \frac{S(t)}{M + S(t)} \quad (3)$$

where $M = \mathrm{HR}_{\mathrm{stress}}/\mathrm{HR}_{\mathrm{rest}} - 1 \approx 0.5$ is the maximum fractional HR elevation under acute psychosocial stress (population prior). The normalised recovery term in Eq. (1) equals 1 immediately after a stressor and approaches 0 as recovery completes.

2.3 Unexpectedness Factor

$$U_i = \frac{|E_i \cdot R_i - \mu_i|}{\sigma_i \cdot \eta_i^{1/4}} \quad (4)$$

E_i is the kinematic error magnitude; R_i is experimenter-assigned: $R_i = 0$ for therapeutic perturbations, $R_i \in$

$\{1, 2, 3\}$ for unintended errors graded by consequence (minor deviation, balance threat, fall risk). A formal rubric is future work; μ_i, σ_i are the running mean and standard deviation of prior stressor magnitudes. The sample-size warmup $\eta_i = \min(n_i, n_{\mathrm{ref}})/n_{\mathrm{ref}}$ dampens U_i before the user's error distribution stabilises; $n_{\mathrm{ref}} = 10$ is heuristic, tuned per subject.

3. Parameter Ranges and Numerical Example

3.1 Parameter ranges

Individual parameters require per-subject fitting; their ranges are verified against existing data. TSST sessions in WESAD [5] yield $M \approx 0.36$–0.43 from $\mathrm{HR}_{\mathrm{rest}} \approx 70$ and $\mathrm{HR}_{\mathrm{stress}} \approx 95$–$100$ bpm; we adopt $M = 0.4$. Cardiac recovery timescales [6] place $T_s \in 5$–8 min, with $T_s = 6$ min retaining $\sim$3.6% of a stressor's weight after 20 min.

3.2 Time-domain example

Fig. 1 simulates Eq. (1) over a 10-min session with $A_{\mathrm{base}} = 35$ (population-typical STAI), $A_{\mathrm{thresh}} = A_{\mathrm{base}} + 8$, $M = 0.40$, $T_s = 6$ min, and three events: a therapeutic perturbation at 1 min ($R = 0$), a mild unintended error at 3 min ($E = 0.6$, $R = 1$), and a larger unintended error at 6 min ($E = 0.9$, $R = 2$). The first error stays sub-threshold; the second crosses A_{thresh} and triggers the controller response in Section 4.

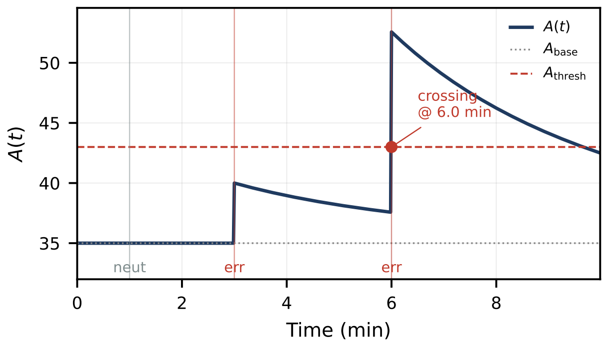

Figure 1: Simulated $A(t)$ for a 10-min session with three events. Neutral perturbation (1 min) contributes zero; first error (3 min) stays sub-threshold; second error (6 min) crosses A_{thresh} (dashed). Exponential recovery follows.

4. Closed-Loop Architecture

Fig. 2 shows the proposed control architecture. Kinematic data (IMU/MoCap) yield E_i, U_i, and R_i; the cardiac HR trace yields $\mathrm{HRS}(t)$ normalised against individually fitted parameters.

The scalar $A(t)$ is compared against an intervention threshold A_{thresh}, set per-individual as a fixed offset above A_{base}. Below threshold, the controller holds. At or above, it applies *increased actuation predictability* (slower ramps, pre-cues, reduced timing jitter), targeting SPE without withdrawing therapeutic load. If $A(t)$ stays above A_{thresh} for $\Delta t_{\mathrm{esc}} = T_s/2 \approx 3$ min, the controller escalates to assistance reduction. EDA, when available, is logged in parallel; principled HR/EDA fusion and disagreement handling are left to future work.

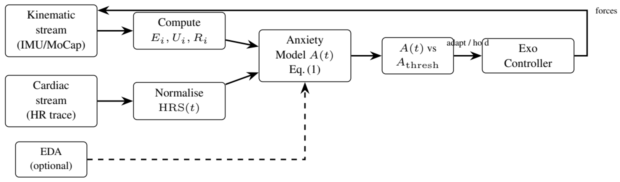

Figure 2: Closed-loop anxiety-mediated control architecture. Kinematic and cardiac streams feed the anxiety model; $A(t)$ drives controller adaptation. EDA (dashed) is an optional logging channel; fusion is future work.

5. Discussion

The model assumes HR is a reliable proxy for SNS activation, with per-subject fitting absorbing individual variation. Because therapeutic exertion is the modal operating condition for rehabilitation exoskeletons, exercise-induced cardiac arousal is the central validity threat to $A(t)$: per-subject HRS normalisation and the EDA channel mitigate this, but exertion-matched controls are essential for formal validation.

6. Conclusion

This paper has presented a closed-form model of state anxiety computable in real time from kinematic and cardiac signals available in wearable HRI systems. A closed-loop controller with access to $A(t)$ can adjust actuation predictability before trust failure, intervening at the mechanism rather than the outcome. Per-subject fitting against VAS-rated anxiety, targeting a moderate-to-strong correlation between predicted and reported values, is the immediate next step.

References

[1] L. Stirling, M. I. Wu, and X. Peng, "Measuring trust for exoskeleton systems," arXiv:2407.07200, 2024.

[2] L. Miller *et al.*, "More than a feeling—Interrelation of trust layers in HRI and the role of user dispositions and state anxiety," *Front. Psychol.*, vol. 12, p. 592711, 2021.

[3] A. Hua *et al.*, "Sensorimotor mismatch disrupts motor automaticity and increases anxiety during a goal-directed balance task," *Front. Hum. Neurosci.*, vol. 19, p. 1632265, 2025.

[4] R. F. Baumeister *et al.*, "Bad is stronger than good," *Rev. Gen. Psychol.*, vol. 5, no. 4, pp. 323–370, 2001.

[5] P. Schmidt *et al.*, "Introducing WESAD, a multimodal dataset for wearable stress and affect detection," in *Proc. ICMI*, pp. 400–408, 2018.

[6] C. Kirschbaum and D. H. Hellhammer, "Salivary cortisol in psychoneuroendocrine research," *Psychoneuroendocrinology*, vol. 19, no. 4, pp. 313–333, 1994.

[7] D. J. Harris *et al.*, "From fear of falling to choking under pressure: A predictive processing perspective of disrupted motor control under anxiety," *Neurosci. Biobehav. Rev.*, vol. 148, p. 105115, 2023.